

A Binary-Quantized Two-Dimensional Cellular Array Model of Linear Diffusion Systems

Hisato Fujisaka, Daisuke Hamano and Takeshi Kamio

Faculty of Information Sciences, Hiroshima City University
3-4-1 Ozukahigashi, Asaminami-ku, Hiroshima 731-3194, Japan
Email: fujisaka@im.hiroshima-cu.ac.jp

Abstract—A binary-quantized two-dimensional cellular array model of linear diffusion systems is investigated microscopically by introducing virtual particles. A simple deterministic rule applied to all the cells of the array determines the motion of the particles in the array. By numerical experiments with the array we found that the virtual particles whose behavior is deterministic possess almost the same characteristics as probabilistic Brownian particles in diffusion systems have.

1. Introduction

Discrete and multi-valued models of distributed parameter systems have been studied for computational physics and digital signal processing.

Two and higher-dimensional linear diffusion systems are modeled by lattice-gas cellular automata (LGCA) [1]. However, application of LGCA is limited because of simple behavior of particles assumed in LGCA models. LGCA have also a problem that they can not be used for modeling one-dimensional diffusion systems.

A new type of binary-quantized one-dimensional cellular array model of linear diffusion systems has been proposed recently [2]. Its macroscopic behavior, that is a diffusion phenomenon, is utilized as a measure of fault tolerance for nanoelectronic circuits [3]. The array may also be used for parallel generation of mutually independent pseudo-random codes by exploiting microscopic similarity between the array and diffusion systems, that is the behavioral similarity between virtual particles assumed in the array and Brownian particles in diffusion systems.

Expanding this useful array into higher dimension is an important work since the expanded array may generate pseudo-random codes of longer period even if simpler operation rule is applied to the cells organizing the array. This paper presents a two-dimensional cellular array and comparison between the array and linear diffusion systems from microscopic points of view.

Table 1: Cell operation.

a(n-1)	b(n-1)	u(n)	v(n)	q(n)
-1	-1	-1	-1	q(n-1)
-1	1	q(n-1)	-q(n-1)	-q(n-1)
1	-1	q(n-1)	-q(n-1)	-q(n-1)
1	1	1	1	q(n-1)

2. Cells and Array Structure

Cells of which two-dimensional (2-D) arrays are composed have two inputs $a(n), b(n)$, two outputs $u(n), v(n)$, and one internal states $q(n)$, all of which take "±1". The cells operate according to Tab. 1.

One-dimensional arrays are built as shown in Fig. 1(a). The 2-D array is built by arranging the 1-D arrays in lattice and connecting them by pairs of cells. Outputs from every two cells in each 1-D array are supplied to their adjacent four cells through the pair of cells as shown in Fig. 1(b). We denote the cell which belongs to j -th row or i -th column array and locates just above or below a pair of cells by $cell_{i,j}^r$ or $cell_{i,j}^c$. Raised indices r, c indicate that the indexed cell belongs to a row or column 1-D array. The inputs and the outputs of $cell_{i,j}^r, cell_{i,j}^c$ are denoted by $a_{i,j}^r(n), \dots, v_{i,j}^c(n)$.

3. Virtual Particles and their Displacement

Figure 2 shows every possible path of a particle moving on one-dimensional axis x by $+\delta$ or $-\delta$ at a probability of $1/2$ for each time interval τ . Suppose that the initial location of the particle is $x = 0$. Then, a probability $p(k, m)$ that the particle locates at $x = \delta k$, at time τm , k, m :integers, is given by

$$p(k, m) = \frac{m!}{\left(\frac{m+k}{2}\right)! \left(\frac{m-k}{2}\right)!} \left(\frac{1}{2}\right)^m \quad (1)$$

The relation between the inputs and the outputs of the cell which operates according to Tab. 1 is expressed by the following simile. Two virtual particles carrying "±1" enter the cell at time $n-1$, pass through

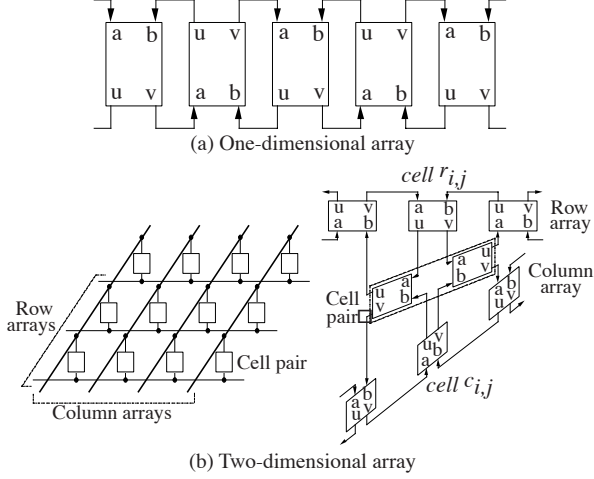


Figure 1: One and two-dimensional cellular arrays.

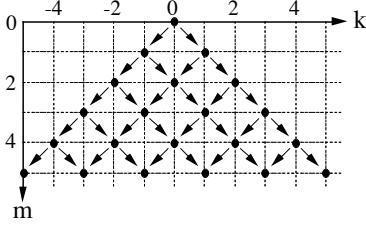


Figure 2: Paths of a random walker

the cell in parallel ($a \rightarrow u, b \rightarrow v$) or cross each other in the cell ($a \rightarrow v, b \rightarrow u$), and go out of the cell at time n . When $a(n) \neq b(n)$, parallel passing or crossing is determined by the following Boolean expression:

$$\text{parallel}/\overline{\text{cross}} = \overline{a(n-1) \oplus q(n-1)} \quad (2)$$

If the values of $a(n)$ and $q(n)$ are "+1/-1", logical "1/0" is given to the corresponding variables in Eq.(2). We assume that cell condition *parallel* or *cross* in case of $a(n) = b(n)$ is also determined by Eq.(2). State $q(n)$ is considered to take "+1" or "-1" at a probability of 1/2 since the state is reversed every time when $a(n) + b(n) = 0$. Then, a probability of parallel passing or crossing is estimated to be 1/2.

In the 1-D array shown in Fig. 1(a), a virtual particle which entered in a cell at time $n-1$ goes out of the cell and enters again into one of its adjacent cells at time n . A probability that the particle moves to the left cell or the right cell is 1/2 because *parallel/cross* takes "1/0" at even probabilities. Although the motion of the particle is deterministic, it is quite similar to the randomly walking particle shown in Fig. 2.

Next, we consider motions of virtual particles on a 2-D array. In Fig. 2, a particle at an even location $2k$ moves to location $2k-2, 2k$, or $2k+2$ for 2τ . Similarly,

in the 2-D array, a particle at $cell_{i,j}^r$ or $cell_{i,j}^c$ moves either to one of three cells $cell_{i+1,j}^r, cell_{i,j}^r, cell_{i-1,j}^r$ in j -th row array or to one of three cells $cell_{i,j+1}^c, cell_{i,j}^c, cell_{i,j-1}^c$ in i -th column array for 3 time steps. In average, the particle is regarded to move both in the row and the column arrays for 6 time steps. Then, a probability $p_r(j, n)$ that a particle in $cell_{0,0}^r$ or in $cell_{0,0}^c$ at time $n=0$ exists in j -th row array at time n is given by

$$p_r(j, n) = p(2j, 2n/6) \quad (3)$$

where n is a multiple of 3. Similarly, a probability $p_c(i, n)$ that the particle exists in i -th column array is given by

$$p_c(i, n) = p(2i, 2n/6) \quad (4)$$

Assume that a motion for each 3-time-step is independent to previous motions. Then, a probability that the particle locates at $cell_{i,j}^r$ or $cell_{i,j}^c$ is given by

$$p_{2D}(i, j, n) = p_r(i, n) \cdot p_c(j, n), \quad n : \text{multiple of } 3 \quad (5)$$

When n is large, above equation is approximated by

$$p_{2D}(i, j, n) \approx \frac{1}{\left(\frac{\pi}{2}\right) \left(\frac{n}{3}\right)} \exp\left(-\frac{4(i^2 + j^2)}{2\frac{n}{3}}\right) \quad (6)$$

The probabilistic distribution (6) has j and i -directional variances σ_r^2 and σ_c^2 given by

$$\sigma_c^2 = \sigma_r^2 = \frac{n}{12} \quad (7)$$

Figure 3 shows numerically obtained probabilistic distributions $p_{2D}(i, j, n), n=1000, 2000$, of virtual particles in a 2-D array. The array is built of 64x64 1-D arrays and given periodic boundary condition. The experimental distributions $p_{2D}(i, j, n)$ are defined as the ratio of a number of particles displaced by i in i -direction and j in j -direction to the total number of particles contained in the array. The experimental distributions agree with theoretically obtained Gaussian distribution (6) whose two-dimensional projections are shown by dotted curves.

By using the experimental distributions, second order moments

$$\begin{aligned} M_{ii} &\approx \sum_i \sum_j i^2 p_{2D}(i, j, n) \\ M_{jj} &\approx \sum_i \sum_j j^2 p_{2D}(i, j, n) \\ M_{ij} &\approx \sum_i \sum_j ij p_{2D}(i, j, n) \end{aligned} \quad (8)$$

are computed. They are shown in Fig. 4. From the figure, we can not state that i -directional and j -directional components of the motion are independent because moment M_{ij} is not zero. The independence will be investigated again in the next section.

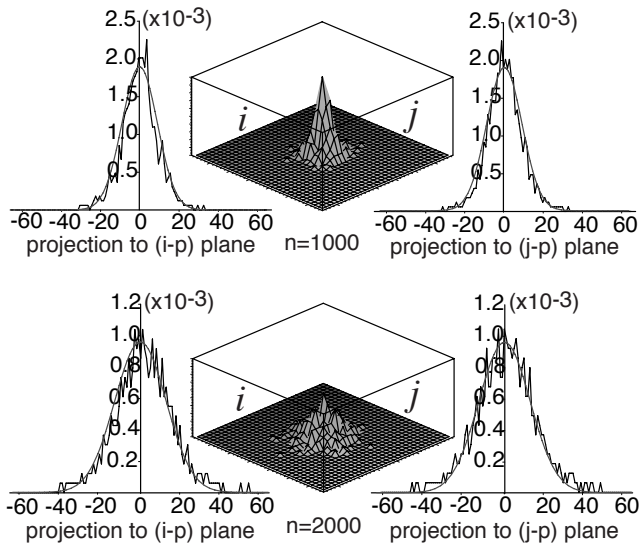


Figure 3: Probabilistic distribution in terms of displacement.

4. Velocity of Virtual Particles

Since the 2-D array is a deterministic system, motion of the virtual particles is periodic after macroscopic diffusion process on the array is in an equilibrium state. Figure 5 shows motions of two particles in an array built of 19x19 1-D arrays. Interestingly, long and complex periodicity is observed even though the array is macroscopically in a trivial equilibrium state. The ratio of the periods of two different motions of two particles is rational.

A particle called Brownian particle has the following properties: (i) Its probabilistic density distribution in terms of displacement is a Gaussian distribution. (ii) variance of the distribution increases in proportion to time. From (i), following property is derived: (iii) In the time domain, the autocorrelation of the average velocity of the particle is a delta function. By the Fourier transform of the autocorrelation, we obtain the following: (iv) In the frequency domain, average velocity has uniform spectral distribution. In the previous section we saw that the virtual particles in a 2-D array have properties (i) and (ii). Then, we expect that the virtual particles also have properties (iii) and (iv).

Velocity of the virtual particles is defined as follows: If a virtual particle at $cell_{i,j}^r$ or $cell_{i,j}^c$ moves to $cell_{i\pm 1,j}^r$ or $cell_{i\pm 1,j}^c$ for 3 time steps, i and j -directional components $v_i(n)$, $v_j(n)$ of its velocity, n :multiple of 3, are given ± 1 and 0 respectively. If the particle moves to $cell_{i,j\pm 1}^r$ or $cell_{i,j\pm 1}^c$, $v_i(n)$, $v_j(n)$ are given 0 and ± 1 . If the particle returns to $cell_{i,j}^r$ or $cell_{i,j}^c$, both of the velocity components are zero.

Numerical analyses of the velocities $v^1(n) = \{v_i^1(n), v_j^1(n)\}$, $v^2(n) = \{v_i^2(n), v_j^2(n)\}$ of the two mo-

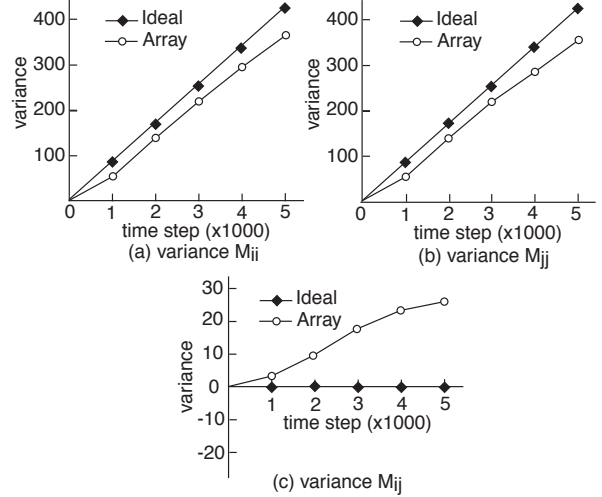


Figure 4: Variances of the probabilistic distribution.

tions in Fig. 5 in both frequency and time domains are shown in Figs. 6 and 7. The spectral density distribution of each velocity component is almost uniform. Autocorrelations $R_{a,dir}(m) \equiv \sum_k v_{dir}^p(3k)v_{dir}^p(3k-m)$, $p = 1, 2$, $dir : i, j$, are like delta functions. Cross correlations between i and j -directional components, $R_{c,ij}(m) \equiv \sum_k v_i^p(3k)v_j^p(3k-m)$, are almost zero. Then, each component of the motion is considered to be independent to another.

Next, we investigate a correlation between velocities of two particles. We use again the two particles whose motions are shown in Fig. 5. The cross correlations $R_c(m) \equiv \sum_k v_{dir1}^1(3k)v_{dir2}^2(3k-m)$, $dir1, dir2 = i, j$, are shown in Fig. 8. The range of the horizontal axes is the greatest common multiple between the periods of the motions of the two particles. The 2-D array may contain a few particles whose motions are relatively identical. If two particle whose motions are different are selected, cross correlation $R_c(m)$ between the two particles is always small as shown in Fig. 8.

5. Conclusions

We have presented a 2-D cellular array and microscopically analyzed its behavior by introducing virtual particles. As a result of the analysis we found that the virtual particles possess almost the same characteristics as Brownian particles have. Moreover, we saw that cross correlations between the velocities of different particles and between two velocity components of one particle are very small. These characteristics imply that the array may be used as a parallel generator of mutually independent pseudo-random codes and the generated codes may be applied to CDMA communications. To investigate the applicability is one of our future works.

References

- [1] D. A. Wolf-Gladrow, "Lattice-Gas Cellular Automata and Lattice Boltzmann Models," *Lecture Notes in Mathematics* 1725, Springer-Verlag, 2000.
- [2] H. Fujisaka and D. Hamano, M. Sakamoto and T. Kamio, "A Binary-Quantized Pseudo-Diffusion System," *Proc. Int'l Symp. on Circuits and Systems, IV*, pp. 720-723, 2004.
- [3] H. Fujisaka, D. Hamano, T. Kamio and M. Sakamoto, "A Fault-Tolerant Architecture for Nanoelectronic Signal Processing," *Proc. IEEE Nanotechnology Conf.*, 2004 (to be published).

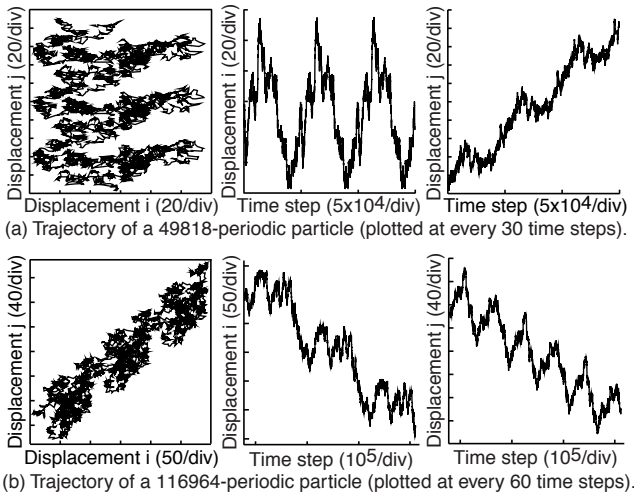


Figure 5: Trajectories of virtual particles in a 19x19 array

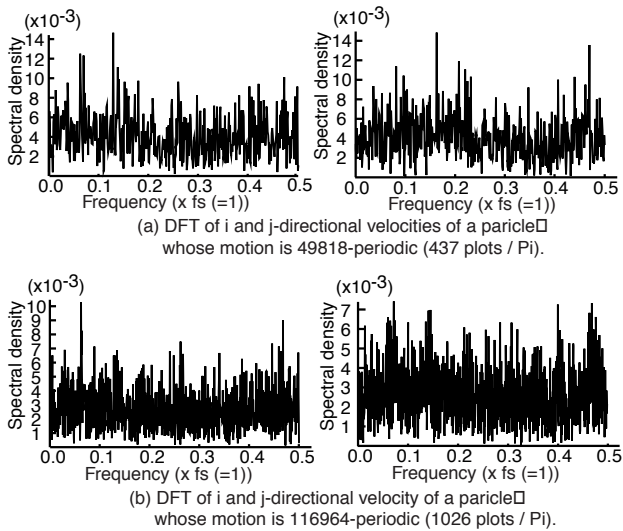


Figure 6: Spectral distribution of the velocities

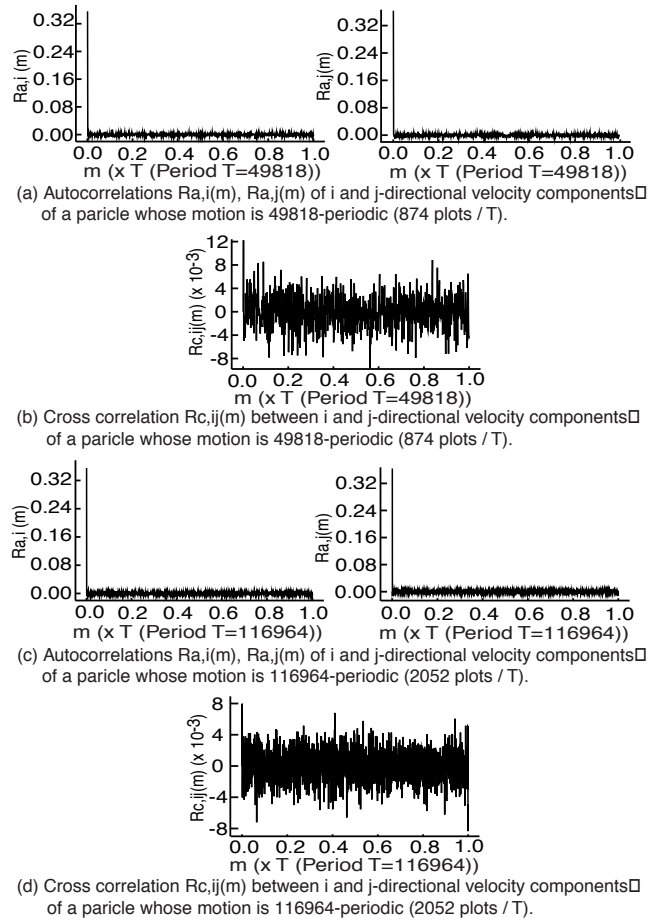


Figure 7: Autocorrelations of the velocity components and cross correlations between i and j -directional components of the velocities.

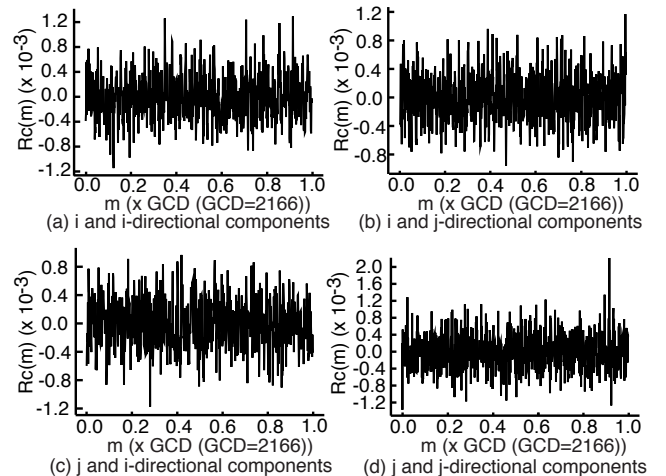


Figure 8: Cross correlations between the velocities of two particles.